A boundary integral equation-discrete wavenumber representation method to study wave propagation in multilayered media having irregular interfaces

Michel Bouchon*, Michel Campillo*, and Stephane Gaffet‡

ABSTRACT

We present a method which combines boundary-integral equation techniques with the discrete wavenumber Green's function representation to study wave propagation in multilayered media having irregular interfaces. The approach is based on the representation of the interfaces by distributions of body forces, the radiation from which is equivalent to the scattered wave field produced by the diffracting boundaries. The Green's functions are evaluated by the discrete wavenumber method. Propagator matrices are introduced to relate force distributions on neighboring interfaces. The solution then requires the inversion of a matrix at each interface. The dimensions of the linear system are independent of the number of layers considered, and the computation time varies linearly with the number of interfaces. We apply the method to calculate surface and vertical seismic profiles in the presence of synclinal or anticlinal structures.

INTRODUCTION

Many problems of wave propagation involving inhomogeneous media can be formulated in terms of boundary-integral equations. The use of this approach, however, lags far behind the use of finite-difference or finite-element techniques. Indeed, the finite-difference and finite-element schemes are often thought of as exclusive tools for calculating the complete solution to problems of wave propagation in laterally varying media. The aim of this paper is to show that the boundary-integral equation formulation may provide an alternate method of calculation.

In the present work, we extend the boundary-integral equation-discrete wavenumber method (Bouchon, 1985; Campillo and Bouchon, 1985; Campillo, 1987) to multiple

irregular interfaces and apply the method to seismic exploration problems. The presentation is restricted to antiplane motion (*SH* waves), which is similar to the acoustic case. The generalization of the scheme to the elastic case, however, is straightforward.

Although the boundary-integral equation formulation for acoustic waves was introduced more than a century ago by Helmholtz and Kirchhoff, use of the method to solve problems of wave propagation in multilayered media has been limited. Previous examples include the works of Larner (1970), Jiracek (1972), and Bard and Tucker (1985), who use the Aki-Larner method, and Dravinski (1983).

DESCRIPTION OF THE METHOD

The problem configuration is depicted in Figure 1. The medium consists of a series of homogeneous layers separated by irregular interfaces. x and z denote the horizontal and vertical directions, respectively. The medium is assumed to be invariant in the direction normal to the (x, z) plane; the free surface is flat; and the seismic source is located at the surface.

The displacement field radiated by a surface force Q_0 with time dependence $e^{i\omega t}$ may be written (Lamb, 1904)

$$u_0(x, z) = \frac{Q_0 e^{i\omega t}}{2\pi i \rho_1 \alpha_1^2} \int_{-\infty}^{\infty} \frac{e^{-i\nu z}}{\nu} e^{-ik(x-x_0)} \, dk, \quad (1)$$

with

$$\nu = [(\omega/\alpha_1)^2 - k^2]^{1/2},$$

where k and ν denote the horizontal and vertical wavenumbers, x_0 is the point of application of the force, and ρ_1 and α_1 are the density and wave velocity in the surface layer.

In order to evaluate the radiated wave field, we introduce a periodicity L in the source-medium configuration. Equation (1) is then replaced by (Bouchon and Aki, 1977)

$$u_0(x, z) = \frac{Q_0 e^{i\omega t}}{iL\rho_1\alpha_1^2} \sum_{n=-M}^{M} \frac{e^{-i\nu_{1,n}z}}{\nu_{1,n}} e^{-ik_n(x-x_0)}, \qquad (2)$$

with

$$k_n = \frac{2\pi}{L} n \quad \text{and} \quad \nu_{1,n} = \left(\frac{\omega^2}{\alpha_1^2} - k_n^2\right)^{1/2}, \quad \text{Im } (\nu_{1,n}) < 0,$$

and M is an integer large enough to ensure the convergence of the series. The substitution of equation (2) for equation (1) replaces the single-source radiation problem, which is difficult to solve, by the numerically simpler problem of evaluating the radiation of a periodic array of sources. As shown by Bouchon and Aki (1977), the single-source, time-domain solution may be later retrieved from the multiple-source result provided that the frequency is chosen to be complex. This choice also removes numerical singularities from equation (2).

We next discretize each interface ℓ into an odd number of points N_ℓ equally spaced along the x direction. At each point i of the interface ℓ, we apply two body forces: $Q_{i\ell 1}e^{i\omega t}$ located on the upper side of the interface radiating into the upper layer and $Q_{i\ell 2}e^{i\omega t}$ situated on the lower side of the interface and radiating into the lower layer. The displacement fields associated with these forces, because of the periodicity introduced, are

$$u_{i,\ell}(x, z) = \frac{Q_{i\ell 1}e^{i\omega t}}{2iL\rho_\ell\alpha_\ell^2} \sum_{n=-\infty}^{\infty} \frac{e^{-i\nu_{\ell,n}|z-z_{i,\ell}|}}{\nu_{\ell,n}} e^{-ik_n(x-x_{i,\ell})} \qquad (3)$$

in the upper layer and in the lower layer

$$u_{i,\ell+1}(x, z) = \frac{Q_{i\ell 2}e^{i\omega t}}{2iL\rho_{\ell+1}\alpha_{\ell+1}^2}$$

$$\times \sum_{n=-\infty}^{\infty} \frac{e^{-i\nu_{\ell+1,n}|z-z_{i,\ell}|}}{\nu_{\ell+1,n}} e^{-ik_n(x-x_{i,\ell})} \qquad (4)$$
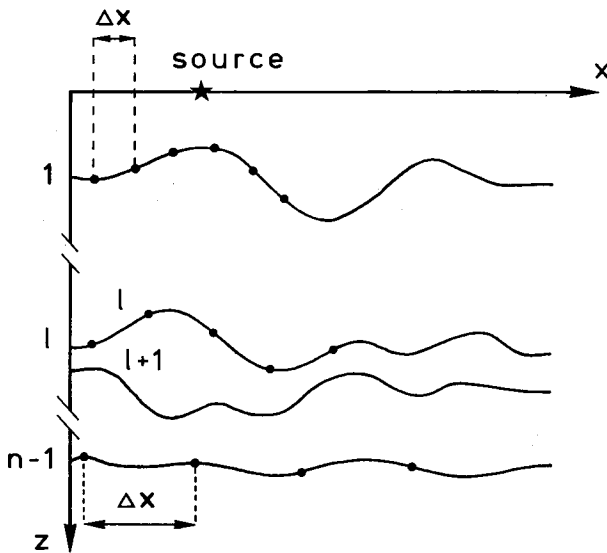

FIG. 1. Problem configuration.

with

$$\nu_{\ell,n} = \left(\frac{\omega^2}{\alpha_\ell^2} - k_n^2\right)^{1/2}, \qquad \text{Im } (\nu_{\ell,n}) < 0,$$

and where $(x_{i,\ell}, z_{i,\ell})$ denotes the x and z coordinates of the discretized interface.

Thus, the total displacement field associated with the force distribution along the interface ℓ in the upper layer is

$$u_\ell(x, z) = \frac{e^{i\omega t}}{2iL\rho_\ell\alpha_\ell^2} \sum_{i=1}^{N_\ell} Q_{i\ell 1}$$

$$\times \sum_{n=-\infty}^{\infty} \frac{e^{-i\nu_{\ell,n}|z-z_{i,\ell}|}}{\nu_{\ell,n}} e^{-ik_n(x-x_{i,\ell})} \qquad (5)$$

and has a similar form in the lower layer. However, because of the existence of both periodicity and discretization in x, equation (5) reduces to (Bouchon, 1985)

$$u_\ell(x, z) = \frac{e^{i\omega t}}{2iL\rho_\ell\alpha_\ell^2}$$

$$\times \sum_{i=1}^{N_\ell} Q_{i\ell 1} \sum_{n=-M_\ell}^{M_\ell} \frac{e^{-i\nu_{\ell,n}|z-z_{i,\ell}|}}{\nu_{\ell,n}} e^{-ik_n(x-x_{i,\ell})}, \qquad (6)$$

with M_ℓ such that $N_\ell = 2M_\ell + 1$.

The discretization in x at equal Δx intervals implies a periodicity in the horizontal wavenumber space, so that the wavenumber summation in equation (6) is restricted to the interval

$$\left[-\frac{\pi}{\Delta x}, \frac{\pi}{\Delta x}\right] \quad \text{or} \quad \left[-\frac{\pi}{L}N_\ell, \frac{\pi}{L}N_\ell\right].$$

The choices of both the periodicity length L and the discretization interval Δx thus uniquely define the sampling of the wavenumber space. The number of terms of the two series in equation (6) is simply $L/\Delta x$. Similarly, in the $\ell + 1$th layer

$$u_{\ell+1}(x, z) = \frac{e^{i\omega t}}{2iL\rho_{\ell+1}\alpha_{\ell+1}^2}$$

$$\times \sum_{i=1}^{N_\ell} Q_{i\ell 2} \sum_{n=-M_\ell}^{M_\ell} \frac{e^{-i\nu_{\ell+1,n}|z-z_{i,\ell}|}}{\nu_{\ell+1,n}} e^{-ik_n(x-x_{i,\ell})}. \qquad (7)$$

We now define the displacement-stress vector at interface ℓ as

$$\mathbf{S}_\ell = [u_\ell(x_{j,\ell}, z_{j,\ell}), j = 1, \ldots N_\ell;$$

$$\sigma_\ell(x_{j,\ell}, z_{j,\ell}), j = 1, \ldots N_\ell]^T, \qquad (8)$$

with

$$\sigma_\ell = \rho_\ell\alpha_\ell^2\left(n_x \frac{\partial u_\ell}{\partial x} + n_z \frac{\partial u_\ell}{\partial z}\right), \qquad (9)$$

where n_x and n_z denote the x and z components of the normal to the interface.

Using equations (6) and (7), we express the displacement-stress field at the ℓth interface as the sum of the contributions from the top side of the ℓth interface (self-interaction

term) and from the underside of the ℓ-1th interface (extrapolated term) in the form (for $\ell \neq 1$)

$$S_\ell = \mathbf{A}_{\ell,1}\mathbf{Q}_{\ell-1,2} + \mathbf{A}_{\ell,2}\mathbf{Q}_{\ell,1}, \tag{10}$$

where the elements of $\mathbf{A}_{\ell,1}$ are

$$a_{j,i}^{\ell,1} = \frac{1}{2iL\rho_\ell\alpha_\ell^2} \sum_{n=-M_{\ell-1}}^{M_{\ell-1}} \frac{e^{-iv_{\ell,n}|z_{j,\ell} - z_{i,\ell-1}|}}{v_{\ell,n}} e^{-ik_n(x_{j,\ell} - x_{i,\ell-1})}$$

and

$$a_{j+N_\ell,i}^{\ell,1} = \frac{-1}{2L}$$

$$\times \sum_{n=-M_{\ell-1}}^{M_{\ell-1}} \left(n_{z_{j,\ell}} \operatorname{sgn}(z_{j,\ell} - z_{i,\ell-1}) + n_{x_{j,\ell}} \frac{k_n}{v_{\ell,n}} \right)$$

$$\times e^{-iv_{\ell,n}|z_{j,\ell} - z_{i,\ell-1}|} e^{-ik_n(x_{j,\ell} - x_{i,\ell-1})},$$

with $\operatorname{sgn}(z_{j,\ell} - z_{i,\ell-1}) = 1$ if $z_{j,\ell} \geq z_{i,\ell-1}$, and $= -1$ otherwise for $j = 1, \ldots N_\ell$ and $i = 1, \ldots N_{\ell-1}$; and the elements of $\mathbf{A}_{\ell,2}$ are

$$a_{j,i}^{\ell,2} = \frac{1}{2iL\rho_\ell\alpha_\ell^2} \sum_{n=-M_\ell}^{M_\ell} \frac{e^{-iv_{\ell,n}|z_{j,\ell} - z_{i,\ell}|}}{v_{\ell,n}} e^{-ik_n(x_{j,\ell} - x_{i,\ell})}$$

and

$$a_{j+N_\ell,i}^{\ell,2} = \frac{-1}{2L} \sum_{n=-M_\ell}^{M_\ell} \left(n_{z_{j,\ell}} \operatorname{sgn}(z_{j,\ell} - z_{i,\ell}) + n_{x_{j,\ell}} \frac{k_n}{v_{\ell,n}} \right)$$

$$\times e^{-iv_{\ell,n}|z_{j,\ell} - z_{i,\ell}|} e^{-ik_n(x_{j,\ell} - x_{i,\ell})},$$

with $\operatorname{sgn}(z_{j,\ell} - z_{i,\ell}) = 1$ if $z_{j,\ell} > z_{i,\ell}$, and $= -1$ otherwise, for $j = 1, \ldots, N_\ell$ and $i = 1, \ldots, N_\ell$.

Because of the continuity of displacement and stress across the interface, we also have

$$S_\ell = \mathbf{B}_{\ell+1,1}\mathbf{Q}_{\ell,2} + \mathbf{B}_{\ell+1,2}\mathbf{Q}_{\ell+1,1}, \tag{11}$$

where the elements of $\mathbf{B}_{\ell+1,1}$ are

$$b_{j,i}^{\ell+1,1} = \frac{1}{2iL\rho_{\ell+1}\alpha_{\ell+1}^2}$$

$$\times \sum_{n=-M_\ell}^{M_\ell} \frac{e^{-iv_{\ell+1,n}|z_{j,\ell} - z_{i,\ell}|}}{v_{\ell+1,n}} e^{-ik_n(x_{j,\ell} - x_{i,\ell})} \quad \text{and}$$

$$b_{j+N_\ell,i}^{\ell+1,1} = \frac{-1}{2L}$$

$$\times \sum_{n=-M_\ell}^{M_\ell} \left[n_{z_{j,\ell}} \operatorname{sgn}(z_{j,\ell} - z_{i,\ell}) + n_{x_{j,\ell}} \frac{k_n}{v_{\ell+1,n}} \right]$$

$$\times e^{-iv_{\ell+1,n}|z_{j,\ell} - z_{i,\ell}|} e^{-ik_n(x_{j,\ell} - x_{i,\ell})},$$

with $\operatorname{sgn}(z_{j,\ell} - z_{i,\ell}) = 1$ if $z_{j,\ell} \geq z_{i,\ell}$, and $= -1$ otherwise, for $j = 1, \ldots N_\ell$ and $i = 1, \ldots N_\ell$ and where the elements of $\mathbf{B}_{\ell+1,2}$ are

$$b_{j,i}^{\ell+1,2} = \frac{1}{2iL\rho_{\ell+1}\alpha_{\ell+1}^2}$$

$$\times \sum_{n=-M_{\ell+1}}^{M_{\ell+1}} \frac{e^{-iv_{\ell+1,n}|z_{j,\ell} - z_{i,\ell+1}|}}{v_{\ell+1,n}} e^{-ik_n(x_{j,\ell} - x_{i,\ell+1})} \quad \text{and}$$

$$b_{j+N_\ell,i}^{\ell+1,2} = \frac{-1}{2L}$$

$$\times \sum_{n=-M_{\ell+1}}^{M_{\ell+1}} \left[n_{z_{j,\ell}} \operatorname{sgn}(z_{j,\ell} - z_{i,\ell+1}) + n_{x_{j,\ell}} \frac{k_n}{v_{\ell+1,n}} \right]$$

$$\times e^{-iv_{\ell+1,n}|z_{j,\ell} - z_{i,\ell+1}|} e^{-ik_n(x_{j,\ell} - x_{i,\ell+1})},$$

with $\operatorname{sgn}(z_{j,\ell} - z_{i,\ell+1}) = 1$ if $z_{j,\ell} > z_{i,\ell+1}$, and $= -1$ otherwise for $j = 1, \ldots, N_\ell$ and $i = 1, \ldots, N_{\ell+1}$.

The continuity of the displacement-stress vector at the deepest interface may be written as

$$S_{n-1} = \mathbf{A}_{n-1,1}\mathbf{Q}_{n-2,2} + \mathbf{A}_{n-1,2}\mathbf{Q}_{n-1,1} = \mathbf{B}_{n,1}\mathbf{Q}_{n-1,2}, \tag{12}$$

which implies

$$\mathbf{Q}_{n-1} = \mathbf{D}_{n-1}^{-1}\mathbf{A}_{n-1,1}\mathbf{Q}_{n-2,2}, \tag{13}$$

where we have defined

$$\mathbf{D}_{n-1} = [-\mathbf{A}_{n-1,2}; \mathbf{B}_{n,1}] \tag{14}$$

and

$$\mathbf{Q}_{n-1} = [\mathbf{Q}_{n-1,1}; \mathbf{Q}_{n-1,2}].$$

Similarly, the force distribution at interface ℓ, $2 \leq \ell \leq n - 2$, may be written in the form

$$\mathbf{Q}_\ell = \mathbf{D}_\ell^{-1}\mathbf{A}_{\ell,1}\mathbf{Q}_{\ell-1,2} \tag{15}$$

with

$$\mathbf{D}_\ell = [-\mathbf{A}_{\ell,2}; \mathbf{B}_{\ell+1,1} + \mathbf{B}_{\ell+1,2}(\mathbf{D}_{\ell+1}^{-1})_1\mathbf{A}_{\ell+1,1}] \tag{16}$$

and where $(\mathbf{D}_{\ell+1}^{-1})_1$ denotes the upper half of the inverse matrix. Equation (15) propagates the force distribution from one interface to the next one.

At the shallowest interface, we have

$$S_1 = \mathbf{A}_{1,2}\mathbf{Q}_{1,1} + S_{s0} = \mathbf{B}_{2,1}\mathbf{Q}_{1,2} + \mathbf{B}_{2,2}\mathbf{Q}_{2,1}, \tag{17}$$

where S_{s0} is the incident displacement-stress vector produced by the source and the elements of $\mathbf{A}_{1,2}$ are

$$a_{j,i}^{1,2} = \frac{1}{2iL\rho_1\alpha_1^2} \sum_{n=-M_1}^{M_1} \frac{1}{v_{1,n}}$$

$$\times \left[e^{-iv_{1,n}|z_{j,1} - z_{i,1}|} + e^{iv_{1,n}(z_{j,1} + z_{i,1})} \right] e^{-ik_n(x_{j,1} - x_{i,1})} \quad \text{and}$$

$$a_{j+N_1,i}^{1,2} = \frac{-1}{2L} \sum_{n=-M_1}^{M_1} \left\{ n_{z_{j,1}} \left[\operatorname{sgn}(z_{j,1} - z_{i,1}) e^{-iv_{1,n}|z_{j,1} - z_{i,1}|} \right. \right.$$

$$\left. + e^{-iv_{1,n}(z_{j,1} + z_{i,1})} \right] + n_{x_{j,1}} \frac{k_n}{v_{1,n}}$$

$$\left. \times \left[e^{-iv_{1,n}|z_{j,1} - z_{i,1}|} + e^{-iv_{1,n}(z_{j,1} + z_{i,1})} \right] \right\} e^{-ik_n(x_{j,1} - x_{i,1})},$$

with sgn $(z_{j,1} - z_{i,1}) = 1$ if $z_{j,1} > z_{i,1}$, and $= -1$ otherwise. From equation (17) we finally get the solution

$$Q_1 = D_1^{-1} S_{s0}, \qquad (18)$$

where D_1 is given by equation (16).

CHOICE OF THE INTERFACE PERIODICITY AND SAMPLING

The interface sampling is mostly a function of the wavelengths present. The shorter the wavelengths, the smaller the required sampling interval. Campillo (1987) found that a discretization rate of three points per wavelength is sufficient to make the numerical noise level negligible. In Figure 2, we present a comparison between the surface displacement profile obtained by the present method for a flat-layered medium and the one calculated by using plane-wave reflection and transmission coefficients. In both cases, a line force is applied at the surface, oriented perpendicular to the line of receivers. The source wave field is expressed by equation (2). The diffracted wave field is calculated by the present method, i.e., by representing each interface by a double distribution of sources. This result is compared to the displacement field obtained by evaluating each plane-wave component of the source radiation [equation (2)] using the reflection and transmission matrices for the different layers. The model consists of four layers overlying a half-space. The frequency of the source is 20 Hz, and the comparison is made over one period of the source-medium configuration.
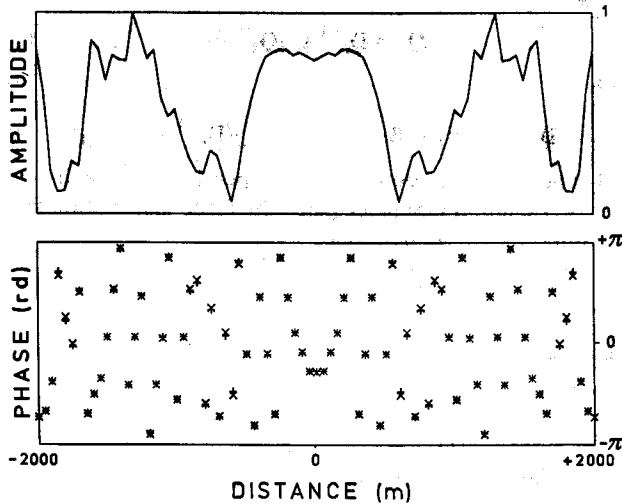

FIG. 2. Comparison of the surface displacement calculated by the boundary-integral equation-discrete wavenumber formulation (x) with the solution obtained by using the flat-layer reflection and transmission coefficients (+). The interfaces are discretized at a rate of two points per shortest wavelength. The model consists of four horizontal layers overlying a half-space. The layer thicknesses are 500, 200, 100, and 200 m. The corresponding wave velocities are 2000, 3000, 2600, 3500 and 4000 m/s with associated densities of 2.0, 2.3, 2.2, 2.4, and 2.5 g/cm³. The source is located at the middle of the distance range considered which is equal to the periodicity interval (4000 m). The frequency considered is 20 Hz plus a small imaginary part equal to one-tenth of the real part.

The discretization interval is different for each interface and is half of the smallest wavelength present on either side of the boundary.

A similar comparison is made in Figure 3 for a sampling rate of three points per wavelength. The remarkable agreement between the two solutions shows the numerical validity of the interface representation and of the propagator matrix scheme. It also confirms that sampling at three points per wavelength is sufficient to ensure the accuracy of the results. At low frequencies (including the static case which is present in the solution before the convolution with the source is performed), we impose, however, a minimum number of points to represent the shape of the interface. In all the applications presented, this minimum value of N_ℓ was arbitrarily choosen to be 41.

The periodicity length L of the source-medium configuration must be chosen according to the simple criterion that no disturbance from a neighboring source or diffracting boundary arrives at the receivers within the time window T considered. The choice of the imaginary part of the frequency has been discussed in previous papers (e.g., Bouchon and Aki, 1977). In all of the applications presented here, the imaginary angular frequency is $-2\pi/T$.

The use of a different sample rate at each interface minimizes computation time by preventing unnecessary sampling of interfaces separating high-velocity formations.

APPLICATIONS

To illustrate the usefulness of our method, we apply it to several exploration configurations. The first application is illustrated in Figure 4. The model is a sine-shaped anticline. The layer and lower half-space velocities are 2500 m/s and 4000 m/s, with corresponding densities of 2.2 g/cm³ and 2.6 g/cm³. The anelastic attenuation of the rocks is introduced in the calculation through the use of slightly dispersive complex wave velocities (e.g., Aki and Richards, 1980). The quality factors used are $Q = 40$ in the surface layer and $Q = 400$ in the half-space. The source is a Ricker wavelet with
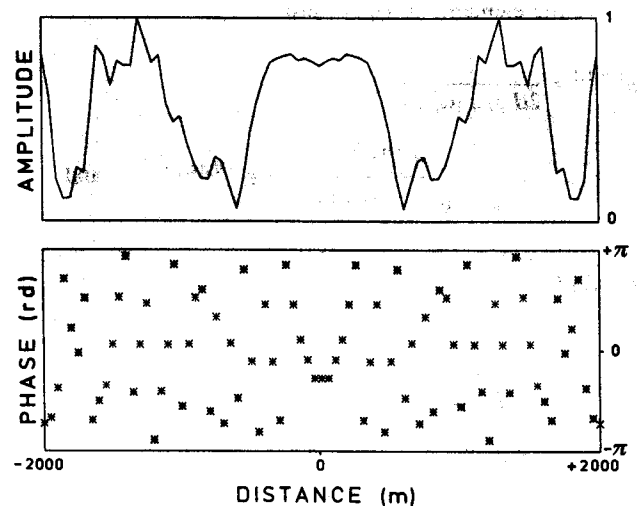

FIG. 3. Same as Figure 2 for an interface sampling rate equal to one-third of the smallest wavelength.

center frequency equal to 25 Hz. The seismograms show the diffracted surface displacement. They display two major arrivals: the first reflection and the first multiple reflection from the top of the anticline.

The second model is a sine-shaped syncline (Figure 5). The surface and half-space velocities are now 2500 m/s and 3000 m/s with corresponding densities of 2.2 g/cm^3 and 2.4 g/cm^3 and quality factors of 40 and 100. The seismograms illustrate the diffracted surface displacement and are characterized by a caustic.

The next example considered (Figure 6) involves a folded anticline. The layer wave velocities are 2500, 3000, 4000, and 5000 m/s with corresponding densities of 2.2, 2.4, 2.6, and 2.7 g/cm^3 and quality factors of 40, 100, 400, and 600. As above, the source emits a Ricker pulse with a 25 Hz center frequency. The diffracted surface displacement seismograms display the primary reflection pulses from the three interfaces. The amplitude of the multiples is very small for this configuration.

The fourth application, displayed in Figure 7, corresponds to a filled sedimentary basin overlying a folded syncline. The layer wave velocities are 2500, 2800, 3000, and 3500 m/s with associated densities of 2.2, 2.3, 2.4, and 2.5 g/cm^3 and quality factors of 40, 80, 100, and 250. The source is the same as the one previously described. The reflections from the

folded layer display the characteristic caustics previously seen in Figure 5.

The final application is the calculation of a vertical seismic profile (VSP) in the model displayed in Figure 7. The recording well is located along the axis of the syncline. The source location is the one indicated in Figure 7. The resulting profile is shown in full scale in Figure 8 and with an amplitude cutoff and independent trace normalization in Figure 9. One interesting feature of the VSP is the apparent splitting of the upgoing and downgoing branches due to the multiplicity of paths for waves reflected by the syncline structure.

CONCLUSION

We have presented a formulation which combines boundary-integral equation techniques with the discrete-wavenumber Green's function representation to calculate the propagation of seismic waves in multilayered media having irregular interfaces. The method is based on a double discretization—in space and in the wavenumber domain—of the integral equations representing the diffracted wave field. The resulting linear system may be decomposed into a combination of layer matrices. The solution then requires the inversion of a matrix at each interface. The method provides a tool for computing surface reflection or refraction profiles and VSPs.
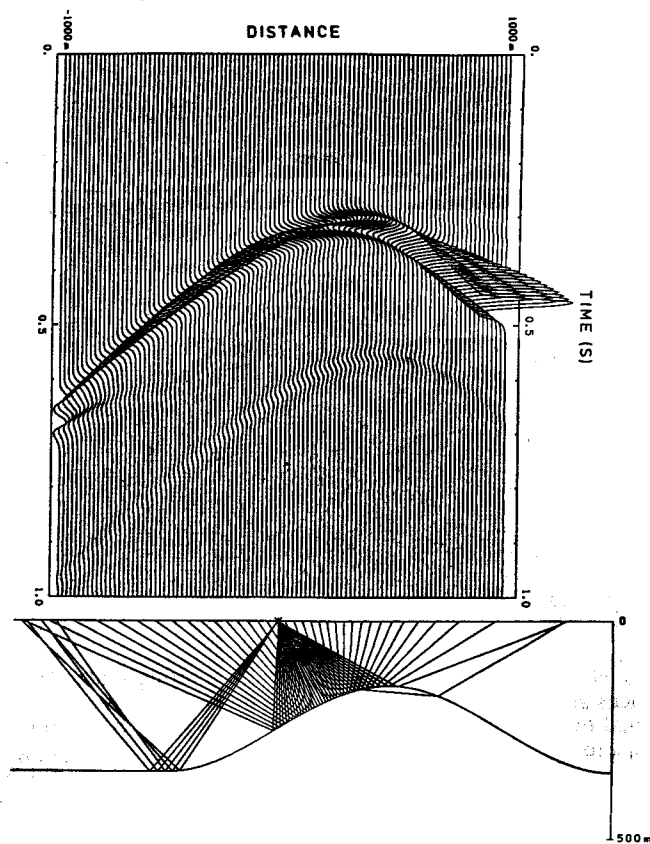

FIG. 4. Diffracted surface displacement and corresponding source-medium configuration. The periodicity length is L = 4000 m.
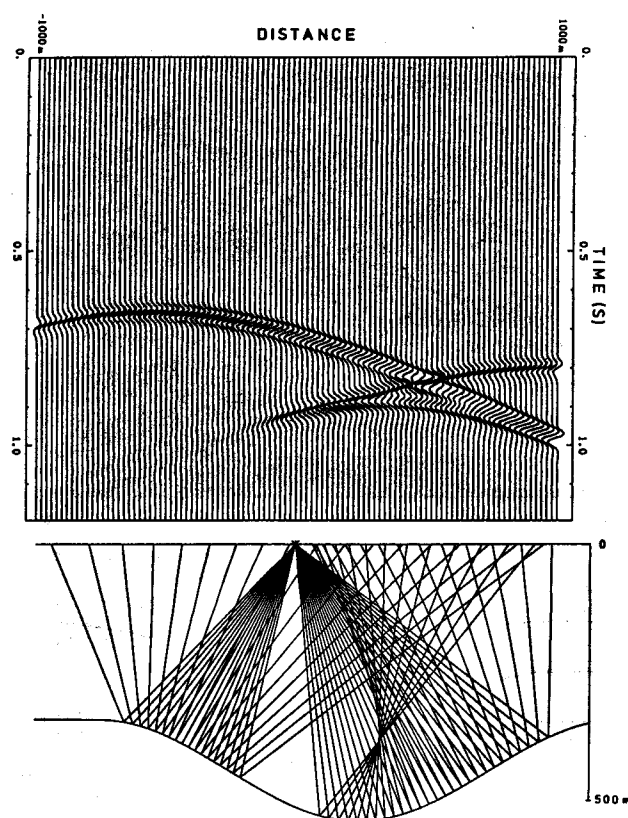

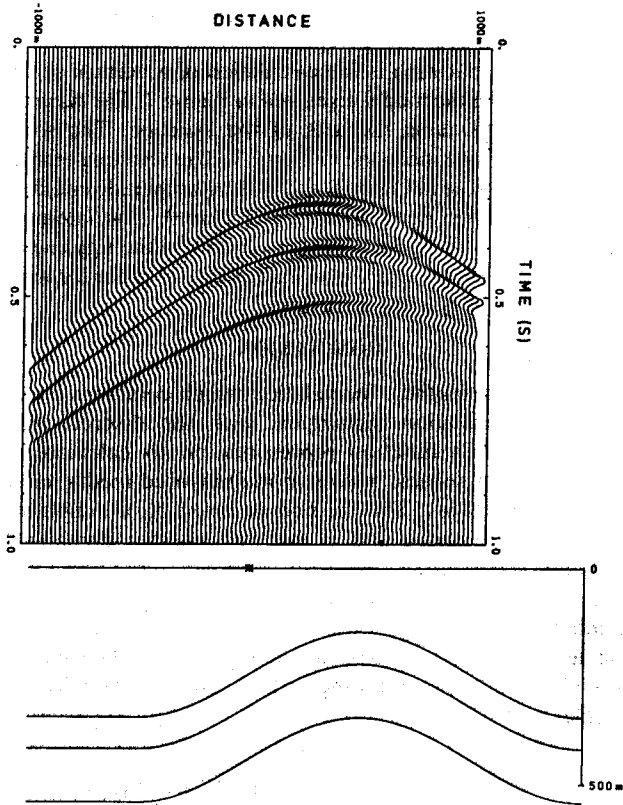FIG. 5. Diffracted surface displacement and corresponding source-medium configuration.

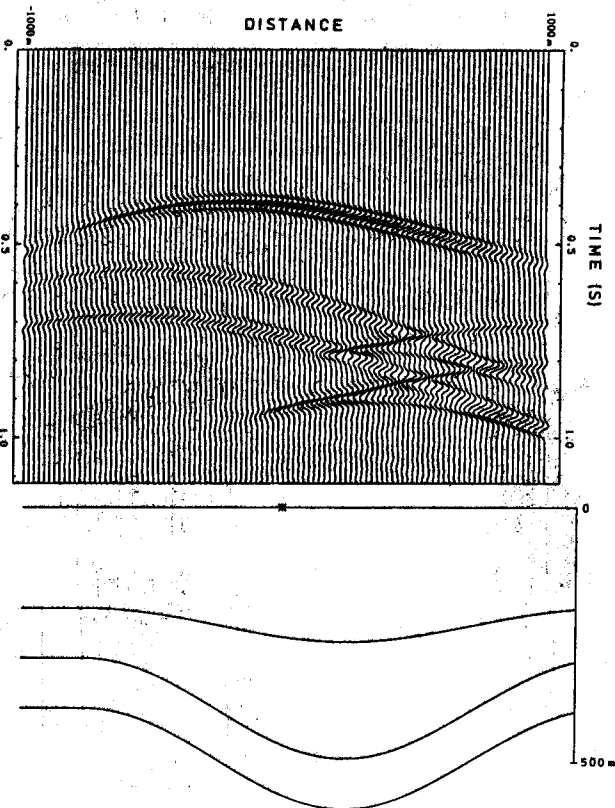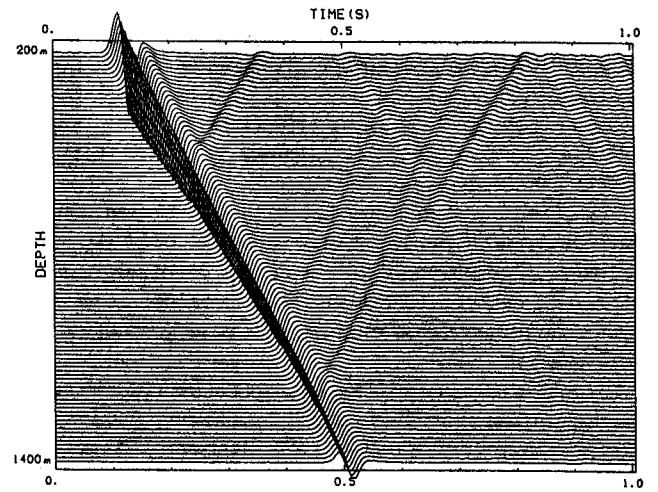FIG. 6. Diffracted surface displacement and corresponding source-medium configuration.

FIG. 8. Vertical seismic profile calculated for the source-medium configuration shown in Figure 7. The recording borehole lies along the axis of the syncline. The source offset is 250 m, and its time dependence is a Ricker pulse of 25 Hz center frequency.
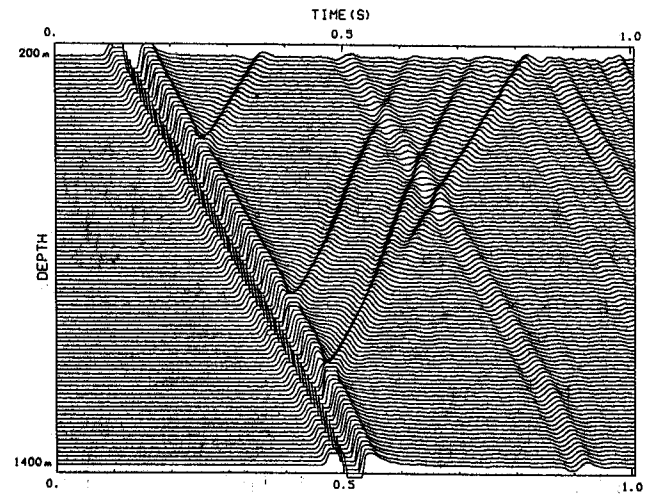

FIG. 7. Diffracted seismogram and corresponding source-medium configuration.

FIG. 9. Same as Figure 8 except for the plotting scale. The traces are normalized independently and an amplitude cutoff equal to one-tenth the maximum amplitude of each signal is applied.

REFERENCES

Aki, K., and Richards, P. G., 1980, Quantitative seismology: Theory and methods: W. H. Freeman and Co.

Bard, P. Y., and Tucker, B. E., 1985, Underground and ridge site effects: a comparison of observation and theory: Bull. Seis. Soc. Am., **75**, 905–922.

Bouchon, M., 1985, A simple, complete numerical solution to the problem of diffraction of SH waves by an irregular interface: J. Acoust. Soc. Am., **77**, 1–5.

Bouchon, M., and Aki, K., 1977, Discrete wavenumber representation of seismic source wave fields: Bull. Seis. Soc. Am., **67**, 259–277.

Campillo, M., 1987, Modeling of SH-wave propagation in an irregularly layered medium—Application to seismic profiles near a dome: Geophys. Prosp., **35**, 236–249.

Campillo, M., and Bouchon, M., 1985, Synthetic SH-seismograms in a laterally varying medium by the discrete wavenumber method: Geophys. J. Roy. Astr. Soc., **83**, 307–317.

Dravinksi, M., 1983, Scattering of plane harmonic SH waves by dipping layers of arbitrary shape: Bull. Seis. Soc. Am., **73**, 1309–1319.

Jiracek, G. R., 1972, Geophysical studies of electromagnetic scattering from rough surfaces and from irregularly layered structures: Ph.D. thesis, Univ. of Cal., Berkeley.

Lamb, H., 1904, On the propagation of tremors at the surface of an elastic solid: Phil. Trans. Roy. Soc. London, **A203**, 1–42.

Larner, K. L., 1970, Near-receiver scattering of teleseismic body waves in layered crust-mantle models having irregular interfaces: Ph.D. thesis, Mass. Inst. of Tech.